Computation of interface reflection and regular or diffuse transmission of the planar symmetric radiative transfer equation with isotropic scattering and its diffusion limit *

Shi Jin, Xiaomei Liao and Xu Yang†

August 2, 2007

Abstract

In this paper, we develop a numerical scheme for the interface problem in the planar symmetric radiative transfer equation with isotropic scattering. Such problems arise in the modeling of the propagation of energy density for waves in heterogeneous media with weak random fluctuation in the high frequency regime. The idea, following the earlier work of Jin and Wen for regular transmission and reflection, is to build the interface condition, which characterizes the reflection and transmission, into the numerical flux. The new contribution of this article is to deal with the *diffuse* transmission at the interface. The positivity of the scheme is proven. Moreover, we show, via numerical examples, that this new scheme is able to capture the correct (regular or diffuse) transmission and reflection through the interface, and, as the mean free path goes to zero, captures the diffusion limit with the correct interface conditions.

1 Introduction

The radiative transfer equation was first proposed [7] by Chandrasekhar and was successfully applied to describe the propagation of light through a turbulent atmosphere. It also arises in semiconductor device modeling, [22], the propagation of energy density for waves in heterogeneous media with weak random fluctuation in the high frequency regime [25], among other applications.

In this paper, we are interested in solving the radiative transfer equation arising in the high frequency limit for scalar wave propagation in a slowly varying background

*Research supported in part by NSF grant Nos. DMS-0305081 and DMS-0608720.

†Department of Mathematics, University of Wisconsin, Madison, WI 53706, USA. Email: jin@math.wisc.edu, liao@math.wisc.edu, xyang@math.wisc.edu.

with small random perturbations [25]. The full model in three dimensional space is given by

$$\frac{\partial a}{\partial t} + v\hat{\mathbf{k}} \cdot \nabla_{\mathbf{x}} a = \int \sigma(\mathbf{x}, \mathbf{k}, \mathbf{k}')\delta(v|\mathbf{k}| - v|\mathbf{k}'|)(a(t, \mathbf{x}, \mathbf{k}') - a(t, \mathbf{x}, \mathbf{k}))\, d\mathbf{k}', \tag{1.1}$$

where the position vector $\mathbf{x} = (x_1, x_2, x_3) \in \mathbf{R}^3$, wave vector $\mathbf{k} = (k_1, k_2, k_3) \in \mathbf{R}^3$, $\hat{\mathbf{k}}$ is the unit vector in the direction $\mathbf{k}$ and $v = 1/\sqrt{\rho\kappa}$ is the background sound speed with ρ the density and κ the compressibility of the background media. $\sigma(\mathbf{x}, \mathbf{k}, \mathbf{k}')$ is the differential scattering cross section and is usually symmetric in $\mathbf{k}$ and $\mathbf{k}'$. δ is the Kronecker delta function.

This radiative transfer equation arises in the high frequency limit of acoustic wave in a random medium (see the survey article [4]), under the following assumption on the random inhomogeneities: (i), the correlation length of the inhomogeneities are comparable to wavelengths, (ii) the fluctuations of the inhomogeneities are weak. Similar radiative transfer equations also arise in high frequency limits of other waves such as elastic or electromagnetic waves in random media, see [25].

We are concerned with the case when the sound speed v contains discontinuities, which will generate interfaces between two different media. As a consequence, waves crossing this interface will undergo (regular or diffuse) transmissions and reflections. It is known from classical mechanics that the Hamiltonian $H = v|\mathbf{k}|$ remains a constant along the particle trajectory. In the case of wave propagation, this corresponds to Snell's Law of Refraction [14].

Here we make some simplifications. Assume that the medium in which waves propagate is planar symmetric. Then Eq.(1.1) can be reduced to a one dimensional transport equation

$$\frac{1}{v}\frac{\partial a}{\partial t} + \mu\frac{\partial a}{\partial x} = \int_{-1}^{1} \sigma(x, \mu, \mu')[a(t, x, \mu') - a(t, x, \mu)]\, d\mu', \tag{1.2}$$

where $x = x_3 \in \mathbf{R}$, $\mu = \hat{k}_3 \in [-1, 1]$. For convenience, we still use the same notation for the new differential scattering across section $\sigma(x, \mu, \mu')$. In this 1D model, the wave vector $\mathbf{k}$ in the 3D model has been switched to $\mu = \hat{k}_3$, which is the cosine value of the polar angle in spherical coordinates. The corresponding Snell's Law of Refraction takes the form:

$$\frac{\sqrt{1-\mu_1^2}}{v_1} = \frac{\sqrt{1-\mu_2^2}}{v_2} \tag{1.3}$$

where μ_1 and μ_2 are respectively the cosines of incidence and transmission angles. μ', the cosine of reflection angle, satisfies $\mu' = -\mu_1$ by the reflection law.

The main idea in the Hamiltonian-preserving schemes for high frequency waves (described by the Liouville equation) through interfaces developed in [13, 15] is to utilize Snell's law and the interface condition that characterize the (regular) transmission and reflection in the numerical flux. This idea will be extended to the 1D model (1.2). The main difference here is in the transmission. Due to the flat or random rough interfaces separating the two media, the transmission or reflection could be significantly regular

or dominantly diffusive[1, 3, 10]. Therefore, the numerical flux needs to be modified in order to incorporate these new interface conditions.

To our knowledge, this is the first numerical method for the radiative transfer equation (1.2) through a *diffusive* interface.

Another difference with the previous works along this line is that, unlike the Liouville equations treated in [13, 15], where the exact solutions can be constructed, one in general cannot find the exact solution for (1.2). On the other hand, when the transport mean free path, which measures the distance between two successive collisions, is small, the diffusion approximation well describes the asymptotic behavior of the radiative transfer equation. To be more specific, we re-scale (1.2) by the scattering mean free path ϵ:

$$\frac{\epsilon^2}{v}\frac{\partial a}{\partial t} + \epsilon\mu\frac{\partial a}{\partial x} = \int_{-1}^{1} \sigma(x,\mu,\mu')[a(t,x,\mu') - a(t,x,\mu)]\, d\mu'. \tag{1.4}$$

When $\epsilon \to 0$, away from the boundary or interface layers, $a(t,x,\mu)$ tends to be isotropic, $a(t,x,\mu) \approx a^{(0)}(t,x)$, where $a^{(0)}(t,x)$ satisfies the diffusion equation [6, 17]:

$$\frac{2}{v}\frac{\partial a^{(0)}}{\partial t} - \frac{\partial}{\partial x}(D\frac{\partial a^{(0)}}{\partial x}) = 0 \tag{1.5}$$

where D is a positive diffusion constant and will be given explicitly later. A boundary layer analysis around the interface gives the interface condition for the diffusion equation (1.5), as was done by Bal and Ryzhik in [2].

As a way to justify the correctness of our numerical method for (1.2) with the interface, we will compare its numerical solution with that of (1.5) with the corresponding interface conditions. To this aim we also need to develop a new numerical method for the diffusion equation with the interface condition, following the immersed interface method, see [23, 24, 19] as well as [21].

This paper is organized as follows. In Section 2, we briefly review the radiative transfer equation in 1D, which is reduced from the full 3D model, and its diffusion limit when the mean free path ϵ is small. Based on the conservation of energy flux, two interface conditions derived in [2] are discussed in Section 3. Numerical schemes are presented in Section 4 for both the radiative transfer equation and diffusion equation with the two different interface conditions corresponding to different transmissions. Positivity of the scheme under a suitable time step restriction is proven. We give some numerical examples in Section 5 to verify the accuracy of our numerical schemes and to compare with the diffusion limits with the corresponding interface conditions with decreasing mean free path. We end the paper in Section 6 with some concluding remarks.

2 Radiative transfer and its diffusion approximation

The radiative transfer equation for the phase space energy density $a(t, \mathbf{x}, \mathbf{k})$ reads

$$\frac{\partial a}{\partial t} + v\hat{\mathbf{k}} \cdot \nabla_{\mathbf{x}} a = \int \sigma(\mathbf{x}, \mathbf{k}, \mathbf{k}')\delta(v|\mathbf{k}| - v|\mathbf{k}'|)(a(t, \mathbf{x}, \mathbf{k}') - a(t, \mathbf{x}, \mathbf{k}))\, d\mathbf{k}',$$
$$\mathbf{x} \in \mathbf{R}^3, \quad \mathbf{k} \in \mathbf{R}^3, \quad \hat{\mathbf{k}} = \mathbf{k}/|\mathbf{k}|, \quad v = 1/\sqrt{\rho\kappa}. \tag{2.1}$$

Here, the differential scattering cross section $\sigma(\mathbf{x}, \mathbf{k}, \mathbf{k}')$ is usually symmetric in $\mathbf{k}$ and $\mathbf{k}'$. If only rotationally invariant scattering is concerned, then $\sigma(\mathbf{x}, \mathbf{k}, \mathbf{k}')$ depends only on the angle between $\mathbf{k}$ and $\mathbf{k}'$, i.e.

$$\sigma(\mathbf{x}, \mathbf{k}, \mathbf{k}') = \sigma(\mathbf{x}, \mathbf{k} \cdot \mathbf{k}'), \tag{2.2}$$

and the total scattering cross-section Σ is

$$\Sigma(\mathbf{x}, \mathbf{k}) = \int \sigma(\mathbf{x}, \mathbf{k}, \mathbf{k}')\, d\mathbf{k}'.$$

The phase space energy flux is given by

$$\mathbf{F}(t, \mathbf{x}) = v \int \hat{\mathbf{k}} a(t, \mathbf{x}, \mathbf{k})\, d\mathbf{k}. \tag{2.3}$$

As in [2], we consider here a planar symmetric medium, which means that the geometry and the physical parameters of the medium are invariant by translation in directions perpendicular to x_3. Then Eq.(2.1) reduces to

$$\frac{\partial a}{\partial t} + v\hat{k_3}\frac{\partial a}{\partial x_3} = \int \sigma(x_3, \mathbf{k} \cdot \mathbf{k}')\delta(v|\mathbf{k}| - v|\mathbf{k}'|)(a(t, x_3, \mathbf{k}') - a(t, x_3, \mathbf{k}))\, d\mathbf{k}'. \tag{2.4}$$

Consider the monochromatic isotropic initial data for (2.4)

$$a(0, x_3, \mathbf{k}) = A_0(x_3, \mu)\delta(v|\mathbf{k}| - \omega), \tag{2.5}$$

where ω is the time frequency.

After performing a variable change $a(t, x_3, \mathbf{k}) = v^2 a(t, x_3, \mu)\delta(v|\mathbf{k}| - \omega)$ with $\mu = \hat{k}_3$ (the notation remains the same after the variable change), $a(t, x, \mu)$ (we use $x = x_3$ for notational convenience) satisfies

$$\frac{1}{v} \cdot \frac{\partial a}{\partial t} + \mu\frac{\partial a}{\partial x} = \int_{-1}^{1} \sigma(x, \mu, \mu')[a(t, x, \mu') - a(t, x, \mu)]\, d\mu', \tag{2.6}$$

with the initial data

$$a(0, x, \mu) \triangleq a_0(x, \mu) = A_0(x, \mu)/v^2, \tag{2.7}$$

where the notation for the scattering cross section σ is still kept the same and it is related to the original one by

$$\sigma(x,\mu,\mu') = \frac{\omega^2}{v^4}\int_0^{2\pi} \sigma\left(x_3, \sqrt{1-\mu^2}\sqrt{1-\mu'^2}\cos\phi + \mu\mu'\right)\, d\phi. \tag{2.8}$$

The total scattering cross section is now given by

$$\Sigma = \int_{-1}^{1} \sigma(x,\mu,\mu')\, d\mu',$$

which is independent of μ because of (2.2) and (2.8), and the normal component of the flux (2.3) is expressed in terms of $a(t,x,\mu)$ as

$$\mathcal{F}(t,x) = 2\pi\omega^2 \int_{-1}^{1} \mu a(t,x,\mu)\, d\mu. \tag{2.9}$$

The diffusion approximation becomes valid when the transport mean free path $l = v/\Sigma$ becomes small. Let $\epsilon = l/L$ where L is the length of the domain, then by rescaling time and space variables by $t \to \epsilon^2 t$ and $x \to \epsilon x$, one can write Eq.(2.6) as

$$\frac{\epsilon^2}{v}\frac{\partial a}{\partial t} + \epsilon\mu\frac{\partial a}{\partial x} = \int_{-1}^{1} \sigma(x,\mu,\mu')[a(t,x,\mu') - a(t,x,\mu)]\, d\mu', \tag{2.10}$$

with the initial data (2.7).

Expanding the solution of (2.10) in powers of ϵ:

$$a(t,x,\mu) = a^{(0)}(t,x,\mu) + \epsilon a^{(1)}(t,x,\mu) + \epsilon^2 a^{(2)}(t,x,\mu) + \cdots \tag{2.11}$$

and inserting this expansion into Eq.(2.10), one can perform the standard analysis as in [6, 17] to obtain, from the leading order:

$$\int_{-1}^{1} \sigma(x,\mu,\mu') a^{(0)}(t,x,\mu')\, d\mu' = \Sigma a^{(0)}(t,x,\mu) \tag{2.12}$$

which implies that $a^{(0)}(t,x,\mu) = a^{(0)}(t,x)$ is independent of μ. Higher order expansions give

$$a^{(1)}(t,x,\mu) = -\frac{\theta(\mu)}{\Sigma}\cdot\frac{\partial a^{(0)}}{\partial x}\,, \tag{2.13}$$

$$\frac{2}{v}\frac{\partial a^{(0)}}{\partial t} - \frac{\partial}{\partial x}(D\frac{\partial a^{(0)}}{\partial x}) = 0\,, \tag{2.14}$$

where $\theta(\mu)$ solves

$$\theta(\mu) - \int_{-1}^{1} \frac{\sigma(\mu,\mu')}{\Sigma}\theta(\mu')\, d\mu' = \mu,$$

and

$$D = \frac{1}{\Sigma} \int_{-1}^{1} \mu\theta(\mu)\, d\mu.$$

Eq.(2.14) is known as the diffusion limit of (2.10). The initial condition for $a^{(0)}$ is given by

$$a^{(0)}(0,x) = \frac{1}{\Sigma} \int_{-1}^{1} \sigma(x,\mu,\mu') a_0(x,\mu')\, d\mu'. \tag{2.15}$$

3 The interface conditions

We consider an interface between the two different media with jump discontinuities of the energy density. The interface conditions for the radiative transfer equation (2.6) arise from the behavior of waves reflected and transmitted at flat or random rough interfaces.

Denote

$$a(t,x,\mu) = \begin{cases} a_1(t,x,\mu) & x > 0, \\ a_2(t,x,\mu) & x < 0, \end{cases}$$

where $a_{1,2}(t,x,\mu)$ are respectively the solutions of (2.6) on the two sides of the interface $x = 0$. (For convenience, time t will be omitted when we discuss the interface conditions in the sequel). We follow the notations in [2] to give the general interface conditions. $X_1 = \mathbf{R}^+$ is the domain for medium 1 with the background sound speed v_1 and density ρ_1. $X_2 = \mathbf{R}^-$ is the domain for medium 2 with the background sound speed v_2 and density ρ_2. $\Gamma_-^1 = [0,1]$ and $\Gamma_-^2 = [-1,0]$ are respectively the sets of wave vectors in the two media pointing *away* from the interface. $\Gamma_+^1 = [-1,0]$ and $\Gamma_+^2 = [0,1]$ are the sets of wave vectors in the two media pointing *toward* the interface. The reflection and transmission operators $R^{ij} : L_\mu^1(\Gamma_+^j) \to L_\mu^1(\Gamma_-^i), i,j = 1,2$, map the functions defined on Γ_+^j onto the functions on Γ_-^j, where the spaces L_μ^p are defined by $L_\mu^p(X) = L^p(X; |\mu| d\mu)$ and R^{ii} correspond to reflection, while R^{ij},$i \neq j$ describe the transmission across the interface.

The interface conditions for the radiative transfer equation (2.6) at $x = 0$ are

$$a_i(0,\mu)|_{\Gamma_-^i} = \sum_{j=1}^{2} R^{ij} \left(a_j(0,\cdot)|_{\Gamma_+^j} \right)(\mu). \tag{3.1}$$

Since the energy flux (2.9) is conserved across the interface $x = 0$, the reflection and transmission operators must satisfy the following condition:

$$\int_{\Gamma_+^i} \mu h(\mu)\, d\mu + \int_{\Gamma_-^i} \mu [R^{ii}(h)](\mu)\, d\mu = \int_{\Gamma_-^j} \mu [R^{ji}(h)](\mu)\, d\mu \tag{3.2}$$

for all functions $h(\mu) \in L_\mu^1(\Gamma_+^i)$. Furthermore, R^{ij}, $i,j = 1,2$ are bounded and positive operators. One can refer to [2] for more assumptions and properties on these operators.

The response operators $\mathcal{R}^i$, $i = 1, 2$ are defined as

$$\mathcal{R}^i : \begin{array}{ll} L^\infty(\Gamma^i_-) & \longrightarrow L^\infty(\Gamma^i_+) \\ a_i|_{\Gamma^i_-} & \longmapsto a_i|_{\Gamma^i_+}, \end{array} \tag{3.3}$$

and, for any function $G \in L^\infty$, they can be expressed in terms of the Chandrasekhar H-function [7] as:

$$\begin{aligned} (\mathcal{R}^1 G)(-\mu) &= \frac{1}{2} H(\mu) \int_0^1 G(\mu') \frac{H(\mu')}{\mu + \mu'} \mu' d\mu', \\ (\mathcal{R}^2 G)(\mu) &= \frac{1}{2} H(\mu) \int_0^1 G(-\mu') \frac{H(\mu')}{\mu + \mu'} \mu' d\mu', \end{aligned} \tag{3.4}$$

for $\mu \in (0, 1)$. Fig. 1 shows how the operators R^{ij} and $\mathcal{R}^i$ work across the interface $x = 0$.

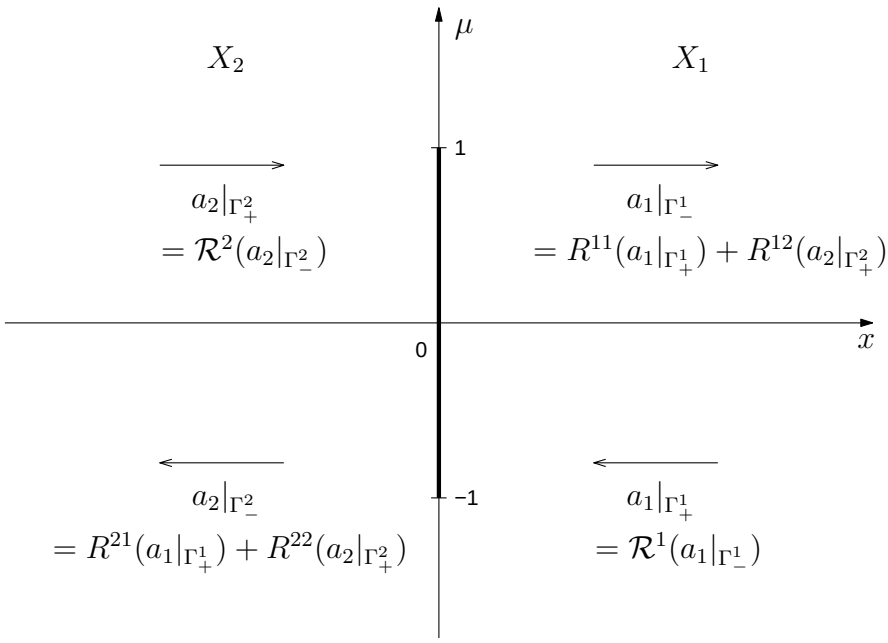

Figure 1: A demonstration for operators R^{ij} and $\mathcal{R}^i$, $i, j = 1, 2$ on the domains X_1, X_2 with the interface at $x = 0$.

We consider two kinds of interface conditions according to different types of interfaces. One is specular reflection with regular transmission as shown in Fig. 2(a), which can be used in practice as an approximation when the interface is flat. The other one is specular reflection and diffuse transmission as shown in Fig. 2(b), where

the transmission operators are isotropically diffusive, which is the more realistic interface condition in the weak randomly fluctuated media with randomly rough interface. We will give explicit expressions for operators R^{ij} under these two types of interface conditions respectively in the following.

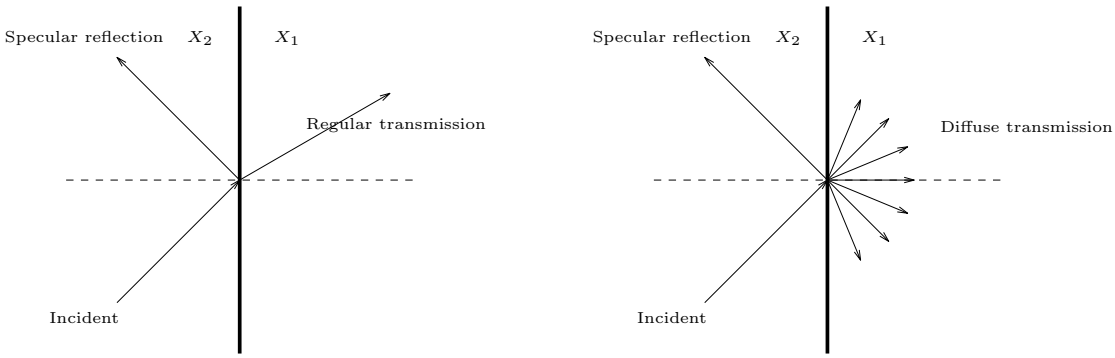

(a) Interface condition I

(b) Interface condition II

Figure 2: A demonstration of interface conditions I and II.

Let μ_1 be the cosine value of the incident angle and μ_2 be the cosine value of the transmission angle. Assume that $\mu_{1,2} > 0$. By Snell's Law of Refraction:

$$\frac{\sqrt{1-\mu_1^2}}{v_1} = \frac{\sqrt{1-\mu_2^2}}{v_2}, \tag{3.5}$$

which can be used to determine μ_2 (cosine of the transmission wave angle) from μ_1 (cosine of the incident wave angle).

- Specular reflection and regular transmission (Interface condition I)

  Assuming $v_1 > v_2$, then the usual Fresnel reflection-transmission coefficients are given by

$$\mathcal{F}^{11}(\mu_1) = \frac{(\rho_2 v_2 \mu_1 - \rho_1 v_1 \mu_2)^2}{(\rho_2 v_2 \mu_1 + \rho_1 v_1 \mu_2)^2}, \quad \mathcal{F}^{21}(\mu_1) = \frac{4\rho_2 \rho_1 v_1^2 \mu_1^2}{(\rho_1 v_1 \mu_2 + \rho_2 v_2 \mu_1)^2},$$

  and

$$\mathcal{F}^{22}(\mu_2) = \mathcal{F}^{11}(\mu_1), \quad \mathcal{F}^{12}(\mu_2) = \frac{4\rho_2 \rho_1 v_2^2 \mu_2^2}{(\rho_1 v_1 \mu_2 + \rho_2 v_2 \mu_1)^2}, \quad \text{if } \mu_2 > \mu_2^c = \sqrt{1 - \frac{v_2^2}{v_1^2}};$$

$$\mathcal{F}^{22}(\mu_2) = 1, \quad \mathcal{F}^{12}(\mu_2) = 0, \quad \text{if } \mu_2 \le \mu_2^c.$$

So the operators R^{ij} in the interface condition (3.1) can be expressed in terms of $\mathcal{F}^{ij}$ as

$$R^{11}(1)(\mu_1) = \mathcal{F}^{11}(\mu_1), \qquad R^{12}(1)(\mu_1) = \frac{\mu_1 v_2}{\mu_2 v_1}\mathcal{F}^{12}(\mu_2), \tag{3.6}$$

$$R^{22}(1)(\mu_2) = \mathcal{F}^{22}(\mu_2), \qquad R^{21}(1)(\mu_2) = \frac{\mu_2 v_1}{\mu_1 v_2}\mathcal{F}^{21}(\mu_1). \tag{3.7}$$

In (3.6), μ_2 is a function of μ_1, and in (3.7), μ_1 is a function of μ_2, both determined from Snell's law (3.5).

One can apply this interface condition on the radiative transfer equation (2.10) in the diffusive regime to give the jump condition of the diffusion equation (2.14). Let

$$a^{(0)}(x,t) = \begin{cases} u_1(x,t), & x > 0, \\ u_2(x,t), & x < 0, \end{cases} \tag{3.8}$$

and

$$D(x,t) = \begin{cases} D_1, & x > 0, \\ D_2, & x < 0, \end{cases} \tag{3.9}$$

then the jump condition for diffusion equation can be expressed as:

$$u_2(0^-) = \alpha u_1(0^+), \tag{3.10}$$

$$D_2 \frac{\partial u_2}{\partial x}(0^-) = D_1 \frac{\partial u_1}{\partial x}(0^+), \tag{3.11}$$

where

$$\alpha = \frac{\|1 - R^{11}(1)\|_{L^1_\mu[0,1]}}{\|1 - R^{22}(1)\|_{L^1_\mu[-1,0]}} = \frac{v_1^2}{v_2^2}. \tag{3.12}$$

Here the values of $a_{1,2}(t,x,\mu)$ for (2.10) on the interface are assumed to be approximately isotropic, so the constant α in (3.12) is independent of the scattering operators inside the media. We are going to use these interface conditions in our numerical computation later. For more details on their derivation and explanation, see [2].

- Specular reflection and diffuse transmission (Interface condition II)

  In this interface condition, the reflection operators are the same as in the previous case, while the transmission operators are isotropically diffusive. Hence

$$R^{11}(a)(\mu_1) = \mathcal{F}^{11}(\mu_1)a(-\mu_1), \qquad R^{12}(a)(\mu_1) = 2\int_0^1 \mu_1 \frac{\mu_1 v_2}{\mu_2 v_1}\mathcal{F}^{12}(\mu_2)a(\mu_2)\, d\mu_1, \tag{3.13}$$

$$R^{22}(a)(-\mu_2) = \mathcal{F}^{22}(\mu_2)a(\mu_2), \qquad R^{21}(a)(-\mu_2) = 2\int_0^1 \mu_2 \frac{\mu_2 v_1}{\mu_1 v_2}\mathcal{F}^{21}(\mu_1)a(-\mu_1)\, d\mu_2. \tag{3.14}$$

There exists an interface layer for the solution of Eq.(2.10) corresponding to this type of interface condition. The resulting interface condition for the diffusion equation (2.14) still has the same form as (3.10) and (3.11) but with a different constant α. To get its new value, one needs to solve an eigenvalue problem posed at the interface. For convenience, using the new notations for the values of the solution $a(t, x, \mu)$ to (2.10) at the interface:

$$a_i^{\pm} = a_i(0, \mu) \quad \text{for} \quad \mu \in \Gamma_{\pm}^i, \quad i = 1, 2,$$

then a_1^- satisfies

$$a_1^- = (I - R^{11}\mathcal{R}^1)^{-1} R^{12}\mathcal{R}^2 (I - R^{22}\mathcal{R}^2)^{-1} R^{21}\mathcal{R}^1 a_1^- \tag{3.15}$$

and a_2^- is given by

$$a_2^- = (I - R^{22}\mathcal{R}^2)^{-1} R^{21}\mathcal{R}^1 a_1^- \tag{3.16}$$

where R^{ij}, $i, j = 1, 2$ are the reflection and transmission operators in (3.1) and $\mathcal{R}^i$, $i = 1, 2$ are the response operators in (3.3).

We summarize briefly the method to get the new α in the following lemmas and theorems which were proven in [2], as a preparation for the later numerical computations.

Lemma 3.1 *Under certain smoothness and bound assumptions as given in [2], there exists a unique normalized solution a_1^- in $L_\mu^1[0, 1]$ of (3.15). Moreover this solution is positive and is bounded away from zero.*

Theorem 3.1 *Let the constants $G_{1,2}$ be defined by $G_1 = G^1(a_1^-)$ and $G_2 = G^2(a_2^-)$, where G^1 and G^2 are given by*

$$G^1(u) = -\frac{1}{D_1\Sigma_1}\left(\int_0^1 \mu\theta(\mu)u(0,\mu)d\mu + \int_{-1}^0 \mu\theta(\mu)\mathcal{R}^1 u(0,-\mu)d\mu\right),$$

$$G^2(u) = -\frac{1}{D_2\Sigma_2}\left(\int_0^1 \mu\theta(\mu)\mathcal{R}^2 u(0,-\mu)d\mu + \int_{-1}^0 \mu\theta(\mu)u(0,\mu)d\mu\right).$$

Then the constants $G_{1,2}$ are positive and the matching constant α is defined as

$$\alpha = \frac{G_2}{G_1}. \tag{3.17}$$

Remark 1 *Note that there is also a theorem in [2] that gives an explicit formula for α. However, it is not easy to use in the numerical computation.*

We will discuss the numerical techniques of calculating α in Section 4.3.

4 Numerical methods

4.1 A finite difference scheme for the radiative transfer equation

We now describe our finite difference scheme for the radiative transfer equation

$$\frac{\partial a}{\partial t} + \frac{1}{\epsilon} v\mu \frac{\partial a}{\partial x} = \frac{1}{\epsilon^2} \int_{-1}^{1} v\sigma(x, \mu, \mu')[a(t, x, \mu') - a(t, x, \mu)]\, d\mu'. \tag{4.1}$$

When we describe the numerical scheme, we consider the two domains connected by the interface as a whole domain instead of considering them separately. So we don not use the notation a_1 and a_2 as in Section 3, instead we discretize the whole domain covering both X_1 and X_2.

We use a uniform mesh with grid points at $x_{i+\frac{1}{2}}$, $i = 0, \cdots, M$, in the $x-$direction and $\mu_{j+\frac{1}{2}}$, $j = 0, \cdots, N$ in the $\mu-$direction. The cells are centered at (x_i, μ_j) with $x_i = \frac{1}{2}(x_{i+\frac{1}{2}} + x_{i-\frac{1}{2}})$ and $\mu_j = \frac{1}{2}(\mu_{j+\frac{1}{2}} + \mu_{j-\frac{1}{2}})$ for $i = 1, \cdots, M$, $j = 1, \cdots, N$. The uniform mesh size is denoted by $\Delta x = x_{i+\frac{1}{2}} - x_{i-\frac{1}{2}}$, $\Delta\mu = \mu_{i+\frac{1}{2}} - \mu_{i-\frac{1}{2}}$. The cell average of a is defined as

$$a_{ij} = \frac{1}{\Delta x \Delta \mu} \int_{x_{i-\frac{1}{2}}}^{x_{i+\frac{1}{2}}} \int_{\mu_{j-\frac{1}{2}}}^{\mu_{j+\frac{1}{2}}} a(x, \mu)\, d\mu\, dx.$$

Assume that the discontinuous points of the sound wave speed $v(x)$ are located at the grid points. Let the left and the right limits of $v(x)$ at point $x_{i+\frac{1}{2}}$ be $v^-_{i+\frac{1}{2}}$ and $v^+_{i+\frac{1}{2}}$ respectively. We approximate $v(x)$ by a piecewise linear function

$$v(x) \approx v^+_{i-1/2} + \frac{v^-_{i+1/2} - v^+_{i-1/2}}{\Delta x}(x - x_{i-1/2})$$

and define the averaged wave speed in a cell by averaging the two cell interface values as $v_i = \frac{1}{2}(v^+_{i-\frac{1}{2}} + v^-_{i+\frac{1}{2}})$. Similarly, we can discretize the differential scattering cross section σ. Typically, σ is constant on both domains X_1 and X_2, so is the total cross section Σ.

The radiative transfer equation (4.1) can be semi-discretized (with time continuous) as

$$(a_{ij})_t + \frac{1}{\epsilon} v_i \mu_j \frac{a^-_{i+\frac{1}{2},j} - a^+_{i-\frac{1}{2},j}}{\Delta x} = \frac{1}{\epsilon^2} \left(\sum_{j=1}^{N} v_i \sigma_{ij} a_{ij} \Delta\mu - v_i \Sigma_i a_{ij} \right). \tag{4.2}$$

Since the characteristics of the radiative transfer equation may be different on the two sides of the interface, the corresponding numerical fluxes should also be different. As in [13, 15], we incorporate into the numerical fluxes $a^-_{i+\frac{1}{2},j}$, $a^+_{i-\frac{1}{2},j}$ the interface condition (3.1). For any regular cells not adjacent to the interface, the numerical fluxes are defined using the regular upwind discretization.

Assume v is discontinuous at $x_{i+\frac{1}{2}}$ and consider the case $\mu_j > 0$. Using upwind scheme, $a^-_{i+\frac{1}{2},j} = a_{ij}$. However, the interface condition (3.1) shows

$$a^+_{i+\frac{1}{2},j} = R^{11}(a(t, x_{i+1}, -\mu^+))(\mu^+) + R^{12}(a(t, x_i, \mu^-))(\mu^+) \tag{4.3}$$

where $\mu^+ = \mu_j$ and μ^- is derived from Snell's law (3.5) by setting $\mu_1 = \mu^+$. Since μ^- may not be a grid point, we have to define it approximately. One can first locate the two cell centers that bound this velocity, and then use a linear interpolation to evaluate the needed numerical flux at μ^-. The case of $\mu_j < 0$ is treated similarly but using the operators R^{22} and R^{21} instead. We will explain the detailed algorithm to generate the numerical flux below. The algorithm will be slightly different for two different types of interface conditions. The difference will be pointed out when needed.

Algorithm

- if $\mu_j > 0$

  $a^-_{i+\frac{1}{2},j} = a_{ij}$, $\mu_{k'} = -\mu_j$

  $\diamond$ if $1 - \left(\frac{v^-_{i+\frac{1}{2}}}{v^+_{i+\frac{1}{2}}}\right)^2 (1-\mu_j^2) > 0$,

  $\mu^- = \sqrt{1 - \left(\frac{v^-_{i+\frac{1}{2}}}{v^+_{i+\frac{1}{2}}}\right)^2 (1-\mu_j^2)}$, $\quad \mu_k \le \mu^- < \mu_{k+1}$ for some integer k.

  Denote

  $$a_{\mu^-} = \frac{\mu_{k+1} - \mu^-}{\Delta\mu} a_{i,k} + \frac{\mu^- - \mu_k}{\Delta\mu} a_{i,k+1},$$

  For interface condition I : using operator (3.6), we have

  $$a^+_{i+\frac{1}{2},j} = R^{11}(1)(\mu_j) a_{i+1,k'} + R^{12}(1)(\mu_j) a_{\mu^-},$$

  For interface condition II : using operator (3.13), we have

  $$a^+_{i+\frac{1}{2},j} = R^{11}(a_{i+1,k'})(\mu_j) + R^{12}(a_{\mu^-})(\mu_j).$$

  $\diamond$ else

  For interface condition I : $a^+_{i+\frac{1}{2},j} = a_{i+1,k'}$.

  For interface condition II : $a^+_{i+\frac{1}{2},j} = a_{i+1,k'} + R^{12}(a_{\mu^-})(\mu_j)$.

  $\diamond$ end

- if $\mu_j < 0$

  $a^+_{i+\frac{1}{2},j} = a_{i+1,j}$, $\mu_{k'} = -\mu_j$

◇ if $1-\left(\frac{v^+_{i+\frac{1}{2}}}{v^-_{i+\frac{1}{2}}}\right)^2(1-\mu_j^2)>0$,

$\mu^+=-\sqrt{1-\left(\frac{v^+_{i+\frac{1}{2}}}{v^-_{i+\frac{1}{2}}}\right)^2(1-\mu_j^2)}$, $\quad \mu_k\le\mu^+<\mu_{k+1}$ for some integer k.

Denote

$$a_{\mu^+}=\frac{\mu_{k+1}-\mu^+}{\Delta\mu}a_{i+1,k}+\frac{\mu^+-\mu_k}{\Delta\mu}a_{i+1,k+1},$$

For interface condition I : using operator (3.7), we have

$$a^-_{i+\frac{1}{2},j}=R^{22}(1)(\mu_j)a_{i,k'}+R^{21}(1)(\mu_j)a_{\mu^+},$$

For interface condition II : using operator (3.14), we have

$$a^-_{i+\frac{1}{2},j}=R^{22}(a_{i,k'})(\mu_j)+R^{21}(a_{\mu^+})(\mu_j).$$

◇ else

For interface condition I : $a^-_{i+\frac{1}{2},j}=a_{i,k'}$.

For interface condition II : $a^-_{i+\frac{1}{2},j}=a_{i,k'}+R^{21}(a_{\mu^+})(\mu_j)$.

◇ end

Remark 2 *In interface condition II, one can discretize the integrals in R^{12} and R^{21} by the direct summation or the trapezoid rule.*

The above algorithm for evaluating numerical fluxes is of first order. One can obtain a second order flux by incorporating a slope limiter, such as the van Leer or minmod slope limiter [18], into the above algorithm. This can be achieved by replacing a_{ij} with $a_{ij}+\frac{\Delta x}{2}s_{ij}$, and replacing $a_{i+1,j}$ with $a_{i+1,j}-\frac{\Delta x}{2}s_{i+1,j}$ in the above algorithm, where s_{ij} is the slope limiter in the x-direction. It is similar in the μ-direction. For the numerical examples in Section 5, we just use the conventional van Leer slope limiter which works well for our examples.

After the spatial discretization is specified, one can use any time discretization for the time derivative.

4.2 Positivity of the scheme

It is also important for a numerical scheme to guarantee the positivity of the energy density $a(t,x,\mu)$ in the radiative transfer equation. We first consider the scheme on (4.1) using the first order numerical flux, and the forward Euler method in time. Assume

that $\mu > 0$ (the case of $\mu < 0$ can be treated similarly with the same conclusion), the scheme becomes

$$\frac{a_{ij}^{n+1} - a_{ij}^n}{\Delta t} + \frac{1}{\epsilon} v_i \mu_j \frac{a_{ij} - a^+_{i-\frac{1}{2},j}}{\Delta x} = \frac{1}{\epsilon^2} \left(\sum_{j=1}^N v_i \sigma_{ij} a_{ij} \Delta\mu - v_i \Sigma_i a_{ij} \right),$$

where

$$a^+_{i-\frac{1}{2},j} = R^{11}(a_{i,k'})(\mu_j) + R^{12}(d_1 a_{i-1,k} + d_2 a_{i-1,k+1})(\mu_j), \quad d_1 + d_2 = 1,$$

with R^{11}, R^{12} positive operators and d_1, d_2 non-negative constants. We omit the superscript n of a. The above scheme can be rewritten as

$$a_{ij}^{n+1} = \left(1 - \frac{1}{\epsilon} v_i \mu_j \frac{\Delta t}{\Delta x} - \frac{\Delta t}{\epsilon^2} v_i \Sigma_i \right) a_{ij} + \frac{\Delta t}{\epsilon^2} \sum_{j=1}^N v_i \sigma_{ij} a_{ij} \Delta\mu + \frac{1}{\epsilon} v_i \mu_j \frac{\Delta t}{\Delta x} a^+_{i-\frac{1}{2},j}. \quad (4.4)$$

To investigate the positivity of scheme (4.4), we just need to prove that if $a_{ij}^n \geq 0$ for all (i, j), then this is also true for a^{n+1}. Clearly one just needs to show that all the coefficients before a^n are non-negative. A sufficient condition for this is

$$1 - \frac{1}{\epsilon} v_i |\mu_j| \frac{\Delta t}{\Delta x} - \frac{\Delta t}{\epsilon^2} v_i \Sigma_i \geq 0,$$

or

$$\Delta t \max_{i,j} \left[\frac{v_i |\mu_j|}{\epsilon \Delta x} + \frac{v_i \Sigma_i}{\epsilon^2} \right] \leq 1. \quad (4.5)$$

Here we need to resolve mean free path ϵ, so $\Delta x = O(\epsilon)$. Hence our scheme needs a time step $\Delta t = O(\epsilon \Delta x) = O(\epsilon^2)$.

Remark 3 *Note that this numerical method is developed for the radiative transfer equation in the regime where $\epsilon = O(1)$. So this ϵ-dependence on Δx and Δt is not a serious problem. When $\epsilon \ll 1$, one could just solve directly the diffusion equation. We keep ϵ here so that we can compare the solution of the radiative transfer equation with the diffusion equation for small ϵ later to verify our method. It is an interesting project to develop numerical methods that allow Δx, Δt independent of ϵ as in [12], which will be a subject of future study.*

Remark 4 *The l^∞ contraction does not hold here as in [11, 13, 14, 15, 16]. This is because of the different interface conditions we use here. In [11, 13, 14, 15, 16], the transmission and reflection coefficients add up to* 1 *since the energy density is conserved at the interface. But here, we conserve the energy flux at the interface, so the coefficients do not necessarily add up to* 1*. In fact, upon some simple algebraic manipulation on (3.6) and (3.7) in interface condition I, one can show that the reflection and transmission operators satisfy the following equality:*

$$R^{11}(1) + R^{12}(1) + \left(\frac{v_2^2}{v_1^2} \right) (R^{22}(1) + R^{21}(1) - 1) = 1. \quad (4.6)$$

In the case of $v_1 > v_2$, we have

$$R^{11}(1) + R^{12}(1) < 1, \tag{4.7}$$

and

$$R^{22}(1) + R^{21}(1) > 1, \tag{4.8}$$

where l^∞ contraction holds only when $\mu > 0$ because R^{11} and R^{12} are used in this situation and they satisfy (4.7). But when $\mu < 0$, we use the coefficients R^{22} and R^{21}, and (4.8) can not guarantee the l^∞ contraction. It is similar for $v_1 < v_2$. Therefore the analytical solution is not l^∞ contraction. It can be easily seen by considering the diffusion limit equation with a constant initial value. Due to the jump condition (3.10), the analytical solution will not remain a constant at the interface. Instead, it goes up on one side and goes down on the other side. However, if one uses an interface condition in which the coefficients adde up to 1, then the analytical solution is l^∞ contraction, so is the numerical scheme.

4.3 The immersed interface method for the diffusion equation

In order to check the correctness of our numerical scheme for the radiative transfer equation, we develop the immersed interface method for the diffusion equation (2.14) using the ideas in [23, 24, 19].

The diffusion approximation of the radiative transfer equation (4.1) when $\epsilon \to 0$ is given by the diffusion equation

$$\frac{2}{v}\frac{\partial a^{(0)}}{\partial t} - \frac{\partial}{\partial x}(D\frac{\partial a^{(0)}}{\partial x}) = 0. \tag{4.9}$$

Using the notation (3.8) and (3.9) in Section 3, we can write Eq.(4.9) in terms of u_i, $i = 1, 2$ in the following ways:

$$\frac{2}{v_i}\frac{\partial u_i}{\partial t} - \frac{\partial}{\partial x}(D_i\frac{\partial u_i}{\partial x}) = 0, \quad i = 1, 2. \tag{4.10}$$

The interface conditions are

$$u_2(t, 0^-) = \alpha u_1(t, 0^+), \tag{4.11}$$

$$D_2\frac{\partial u_2}{\partial x}(t, 0^-) = D_1\frac{\partial u_1}{\partial x}(t, 0^+). \tag{4.12}$$

Therefore

$$\frac{\partial u_2}{\partial t}(t, 0^-) = \alpha\frac{\partial u_1}{\partial t}(t, 0^+), \tag{4.13}$$

$$D_2\frac{\partial^2 u_2}{\partial x \partial t}(t, 0^-) = D_1\frac{\partial^2 u_1}{\partial x \partial t}(t, 0^+). \tag{4.14}$$

Plugging (4.13) into (4.10), one gets the second derivative condition at the interface,

$$v_2 D_2 \frac{\partial^2 u_2}{\partial x^2}(t, 0^-) = \alpha v_1 D_1 \frac{\partial^2 u_1}{\partial x^2}(t, 0^+). \tag{4.15}$$

Differentiating (4.10) once and substituting (4.14) into it, one has the third derivative condition at the interface,

$$v_2 D_2^2 \frac{\partial^3 u_2}{\partial x^3}(t, 0^-) = v_1 D_1^2 \frac{\partial^3 u_1}{\partial x^3}(t, 0^+). \tag{4.16}$$

Once we determined the physically relevant jump conditions, we can begin to develop an immersed interface method to solve it. We use a uniform grid with points $x_i, i = 0, 1, \cdots, N$ and assume that $x_j \le 0 \le x_{j+1}$ for some j. We also assume that the initial and boundary data are specified in such a way that the solution is smooth away from the interface, so we can use a standard finite difference method for the constant coefficient diffusion equation at all grid points except x_j and x_{j+1}. For example, we might use the forward Euler method for time and the central difference for space:

$$\frac{2}{v_i}\frac{U_i^{n+1,l} - U_i^{n,l}}{\tau} - D_i \frac{U_i^{n,l+1} - 2U_i^{n,l} + U_i^{n,l-1}}{h^2} = 0,$$

where $U_i^{n,l} = u_i(t_n, x_l)$, τ is the time step and h is the space step. Note that $0 \le l \le N$ but $l \ne j, j+1$.

Now denote the distance from the interface $x = 0$ to the cell point x_{j+1} by kh where $0 \le k \le 1$. Then the distance from the interface to x_j is $(1-k)h$. We set up a second order difference for $u_2''(x_j)$ and $u_1''(x_{j+1})$ in the following steps.

First, expand $u_1(x_{j+1})$ on x_j with the information of $u_2(x_i)$ by using the interface conditions (4.11) (4.12) (4.15) and (4.16). For convenience, we ignore the time notation here and denote $' = \frac{\partial}{\partial x}$, then

$$\begin{aligned}
u_1(x_{j+1}) &= u_1(0) + khu_1'(0) + \frac{(kh)^2}{2}u_1''(0) + \frac{(kh)^3}{6}u_1'''(0) + O(h^4) \\
&= \frac{1}{\alpha}u_2(0) + kh\frac{D_2}{D_1}u_2'(0) + \frac{(kh)^2}{2}\frac{v_2 D_2}{v_1 \alpha D_1}u_2''(0) + \frac{(kh)^3}{6}\frac{v_2 D_2^2}{v_1 D_1^2}u_2'''(0) + O(h^4) \\
&= \frac{1}{\alpha}(u_2(x_j) + (1-k)hu_2'(x_j) + \frac{((1-k)h)^2}{2}u_2''(x_j) + \frac{((1-k)h)^3}{6}u_2'''(x_j)) \\
&\quad + kh\frac{D_2}{D_1}(u_2'(x_j) + (1-k)hu_2''(x_j) + \frac{((1-k)h)^2}{2}u_2'''(x_j)) \\
&\quad + \frac{(kh)^2}{2}\frac{v_2 D_2}{v_1 \alpha D_1}(u_2''(x_j) + (1-k)hu_2'''(x_j)) \\
&\quad + \frac{(kh)^3}{6}\frac{v_2 D_2^2}{v_1 D_1^2}u_2'''(x_j) + O(h^4).
\end{aligned}$$

Rewrite $u_1(x_{j+1})$ as

$$u_1(x_{j+1}) = \bar{A}u_2(x_j) + \bar{B}u_2'(x_j) + \bar{C}u_2''(x_j) + \bar{D}u_2'''(x_j) + O(h^4), \tag{4.17}$$

where

$$\begin{aligned}
\bar{A} &= \frac{1}{\alpha}, \qquad \bar{B} = \frac{(1-k)h}{\alpha} + kh\frac{D_2}{D_1}, \\
\bar{C} &= \frac{1}{\alpha}\cdot\frac{((1-k)h)^2}{2} + kh\frac{D_2}{D_1}(1-k)h + \frac{(kh)^2}{2}\frac{v_2D_2}{v_1\alpha D_1}, \\
\bar{D} &= \frac{1}{\alpha}\cdot\frac{((1-k)h)^3}{6} + kh\frac{D_2}{D_1}\frac{((1-k)h)^2}{2} + \frac{(kh)^2}{2}\frac{v_2D_2}{v_1\alpha D_1}(1-k)h + \frac{(kh)^3}{6}\frac{v_2D_2^2}{v_1D_1^2}.
\end{aligned}$$

To verify the coefficients, let $\alpha = 1$ and $D_1 = D_2$, then $\bar{A} = 1$, $\bar{B} = h$, $\bar{C} = \dfrac{h^2}{2}$ and $\bar{D} = \dfrac{h^3}{6}$ which are consistent with the case when there is no interface.

Denote $u_2''(x_j) = \delta_0^2 u_2(x_{j-2}) + \delta_1^2 u_2(x_{j-1}) + \delta_2^2 u_2(x_j) + \delta_3^2 u_1(x_{j+1}) + O(h^2)$, then by the Taylor expansion of $u_2(x_{j-2})$, $u_2(x_{j-1})$ and $u_1(x_{j+1})$ on x_j, one needs to solve the linear system (4.18) to get δ_0^2, δ_1^2, δ_2^2 and δ_3^2 where $\bar{A}$, $\bar{B}$, $\bar{C}$ and $\bar{D}$ are given by (4.17),

$$\begin{pmatrix} 1 & 1 & 1 & \bar{A} \\ -2h & -h & 0 & \bar{B} \\ 2h^2 & \frac{1}{2}h^2 & 0 & \bar{C} \\ -\frac{4}{3}h^3 & -\frac{1}{6}h^3 & 0 & \bar{D} \end{pmatrix} \begin{pmatrix} \delta_0^2 \\ \delta_1^2 \\ \delta_2^2 \\ \delta_3^2 \end{pmatrix} = \begin{pmatrix} 0 \\ 0 \\ 1 \\ 0 \end{pmatrix}. \tag{4.18}$$

Similarly, one can expand $u_2(x_j)$ on x_{j+1} with the information of $u_1(x_{j+1})$ by using the interface conditions (4.11) (4.12) (4.15) and (4.16). After denoting $u_1''(x_{j+1}) = \delta_0^1 u_1(x_{j+3}) + \delta_1^1 u_1(x_{j+2}) + \delta_2^1 u_1(x_{j+1}) + \delta_3^1 u_2(x_j) + O(h^2)$, one can get δ_0^1, δ_1^1, δ_2^1 and δ_3^1 by solving (4.19),

$$\begin{pmatrix} 1 & 1 & 1 & \tilde{A} \\ 2h & h & 0 & \tilde{B} \\ 2h^2 & \frac{1}{2}h^2 & 0 & \tilde{C} \\ \frac{4}{3}h^3 & \frac{1}{6}h^3 & 0 & \tilde{D} \end{pmatrix} \begin{pmatrix} \delta_0^1 \\ \delta_1^1 \\ \delta_2^1 \\ \delta_3^1 \end{pmatrix} = \begin{pmatrix} 0 \\ 0 \\ 1 \\ 0 \end{pmatrix}, \tag{4.19}$$

where

$$\begin{aligned}
\tilde{A} &= \alpha, \qquad \tilde{B} = -\left[kh\alpha + (1-k)h\frac{D_1}{D_2}\right], \\
\tilde{C} &= \alpha\cdot\frac{(kh)^2}{2} + (1-k)h\frac{D_1}{D_2}kh + \frac{((1-k)h)^2}{2}\frac{v_1\alpha D_1}{v_2D_2}, \\
\tilde{D} &= -\left[\alpha\cdot\frac{(kh)^3}{6} + (1-k)h\frac{D_1}{D_2}\frac{(kh)^2}{2} + \frac{((1-k)h)^2}{2}\frac{v_1\alpha D_1}{v_2D_2}kh + \frac{((1-k)h)^3}{6}\frac{v_1D_1^2}{v_2D_2^2}\right].
\end{aligned}$$

So if one still uses the forward Euler method for time, then the difference scheme at points x_j and x_{j+1} is given by

$$\frac{2}{v_2}\frac{U_2^{n+1,j}-U_2^{n,j}}{\tau} - D_2(\delta_0^2 U_2^{n,j-2} + \delta_1^2 U_2^{n,j-1} + \delta_2^2 U_2^{n,j} + \delta_3^2 U_1^{n,j+1}) = 0,$$

$$\frac{2}{v_1}\frac{U_1^{n+1,j+1}-U_1^{n,j+1}}{\tau} - D_1(\delta_0^1 U_1^{n,j+3} + \delta_1^1 U_1^{n,j+2} + \delta_2^1 U_1^{n,j+1} + \delta_3^1 U_2^{n,j}) = 0,$$

where $U_i^{n,l} = u_i(t_n, x_l)$, τ is the time step and h is the mesh size.

Remark 5 *The same immersed interface scheme also works when there are source terms in the diffusion equation. However, one needs to change the interface condition to account for the source terms. For example, consider the diffusion equation (4.10) with source terms,*

$$\frac{2}{v_i}\frac{\partial u_i}{\partial t} - \frac{\partial}{\partial x}(D_i\frac{\partial u_i}{\partial x}) + \Sigma_i u_i = 0, \quad i = 1, 2. \tag{4.20}$$

Then plug (4.13) into (4.20), one has

$$\frac{v_2}{v_1\alpha} = \frac{D_1\frac{\partial^2 u_1}{\partial x^2} - \Sigma_1 u_1}{D_2\frac{\partial^2 u_2}{\partial x^2} - \Sigma_2 u_2}. \tag{4.21}$$

Similarly, the third derivative interface condition (4.16) is changed to

$$\frac{D_2 v_2}{D_1 v_1} = \frac{D_1\frac{\partial^3 u_1}{\partial x^3} - \Sigma_1\frac{\partial u_1}{\partial x}}{D_2\frac{\partial^3 u_2}{\partial x^3} - \Sigma_2\frac{\partial u_2}{\partial x}}. \tag{4.22}$$

One can use (4.11), (4.12), (4.21) and (4.22) to get a similar second order approximation for $u_2''(x_j)$ and $u_1''(x_{j+1})$. We omit the details here.

4.4 Computing the coefficient α for interface condition II

We now describe the computation of α for interface condition II. First, we discretize the operators R^{ij} and $\mathcal{R}^i$, $i, j = 1, 2$, numerically by the Gauss quadrature. Note that the Gauss quadrature will provide a higher accuracy in the computation of the Chandrasekhar H-function. Since the operators are linear in interface condition II, the discrete forms of the operators will be constant matrices. Denote the constant matrix A^{ij} to be the discrete form of R^{ij} and the constant matrix B^i to be the discrete form of $\mathcal{R}^i$, then the discrete form of $(I - R^{11}\mathcal{R}^1)^{-1}R^{12}\mathcal{R}^2(I - R^{22}\mathcal{R}^2)^{-1}R^{21}\mathcal{R}^1$ in (3.15) is simply given by $(I - A^{11}B^1)^{-1}A^{12}B^2(I - A^{22}B^2)^{-1}A^{21}B^1$. Similarly, the discrete form of $(I - R^{22}\mathcal{R}^2)^{-1}R^{21}\mathcal{R}^1$ in (3.16) is given by $(I - A^{22}B^2)^{-1}A^{21}B^1$.

After that, we solve the eigenvalue problem (3.15) to get a_1^-, which is the eigenvector corresponding to the eigenvalue of 1, by the power method or the Matlab subroutine *eig*. Finally, one can have a_2^- by plugging a_1^- into (3.16). There exists a steep jump in the eigenvalue a_2^- due to interface condition II. So one needs a very small mesh size to compute a_2^- and we use 512 mesh points here. Please refer to [2] about the graphs of a_1^- and a_2^-, which will not be displayed here although we reproduce them by our computation.

In addition, one should be careful when discretizing R^{12} and R^{21}, because they map the discretized function values on μ_k, $k = 1, \cdots, 512$, into the ones that are not one of μ_k's. Therefore one needs to do interpolation during the discretization. However, it can be avoided by rewriting the expressions of R^{12}, R^{21} as the following

$$\begin{aligned} R^{12}(a)(\mu_1) &= 2\int_0^1 \mu_1 R_0^{12}(a)(\mu_2)\, d\mu_1 = \int_0^1 R_0^{12}(a)(\mu_2)\, d\mu_1^2 \\ &\overset{(*)}{=} \int_0^1 R_0^{12}(a)(\mu_2)\, d\left(\frac{v_1^2}{v_2^2}\mu_2^2\right) = 2\frac{v_1^2}{v_2^2}\int_0^1 \mu_2 R_0^{12}(a)(\mu_2)\, d\mu_2, \end{aligned}$$

and similarly,

$$R^{21}(a)(\mu_2) = 2\frac{v_2^2}{v_1^2}\int_0^1 \mu_1 R_0^{21}(a)(\mu_1)\, d\mu_1,$$

where $R_0^{12}(a)$ and $R_0^{21}(a)$ stand for the transmission operators in (3.6) (3.7) for interface condition I. The equality $(*)$ is the result of Snell's law (3.5).

5 Numerical examples

In this section, we present numerical results to check the performance of the schemes described above. In our computation, we consider an isotropic scattering in each domain. The interface of two domains is located at $x = 0$. The medium on the right half plane X_1 has the density $\rho_1 = 0.5$, the velocity $v_1 = 1.2$, the medium on the left half plane X_2 has the density $\rho_2 = 1.0$, the velocity $v_2 = 1.0$. We are going to conduct the numerical tests using different initial data and different constants for the scattering cross section. The numerical results will be given in terms of two different interface conditions.

Example 1 $\sigma_1(\mu, \mu') = \sigma_2(\mu, \mu') = \frac{1}{2}$, $\Sigma_1 = \Sigma_2 = 1$. *The initial condition of the radiative transfer equation (4.1) is given by*

$$a(0, x, \mu) = \frac{1}{0.03\pi}\exp\left[-(\frac{x}{0.03})^2 - (\frac{\mu}{0.3})^2\right], \tag{5.1}$$

and the corresponding initial data for the diffusion equation (4.9) is

$$\begin{aligned} a^{(0)}(0, x) &= \frac{1}{2}\int_{-1}^1 a(0, x, \mu)\, d\mu \\ &\cong \frac{10}{2\sqrt{\pi}}\exp(-(\frac{x}{0.03})^2). \end{aligned} \tag{5.2}$$

Note: The last equality above holds exactly only when the integral is from $-\infty$ to ∞. The error caused by it is pretty small because it decays almost to 0 out of $[-1,1]$ in the μ-direction.

For numerical computation of the radiative transfer equation (4.1), we use the second order Runge-Kutta for time discretization and the second order flux with the van Leer slope limiter for spatial discretization. The computational domain is chosen as $(x,\mu) \in [-3,3]\times[-1,1]$. Here the domain for x is chosen to be big enough so that the Gaussian initial data decays almost to 0 on the boundary and it provides enough space for the quick diffusion of $a(t,x,\mu)$ when time evolves. So it is convenient for us to use the periodic boundary condition in the x-direction. The mesh we use in the computation under the interface condition I is $M\times N = 1200\times 400$, which means $\Delta x = \Delta\mu = 1/200$. We choose the time step as $\Delta t = \epsilon\Delta x/3$, where the values of ϵ vary from 0.01 to 0.1. Here ϵ needs to be numerically resolved so we should choose $\Delta x < \epsilon$.

We use the same domain and grid points for x in the computation of the diffusion equation (4.9). The first order forward Euler method is used for time discretization and the second order center difference for spatial discretization. The time step is chosen to be $\Delta t = (\Delta x)^2/4$. The jump condition α in this example is given as $\alpha = v_1^2/v_2^2 = 1.44$ for interface condition I and $\alpha = 1.3539$ for interface condition II by solving for a_i^- and using (3.17). Note that α only depends on v, not on ρ, for interface condition I. But for the interface condition II, α does depend on both v and ρ. Although both interface conditions involve ρ and v, the effect of ρ disappears when ϵ goes to 0 for interface condition I but the effect does exist for interface condition II. We ckecked this in our numerical expeiments by varying the value of ρ but will not display this comparison here.

Figs. 3 - 5 display the numerical results using interface condition I. Fig. 3 shows the 3D plot of energy density $a(t,x,\mu)$ of Eq. (4.1) at $t = 0.1$, $\epsilon = 0.03$, which is isotropic in the μ-direction because of the use of interface condition I. We display the result of the average density $\bar{a}(t,x) = \frac{1}{2}\int_{-1}^{1} a(t,x,\mu)\,d\mu$ in Fig. 4 for different values of ϵ. The convergence to its diffusion limit as $\epsilon \to 0$ can be observed here. A zoomed-in image is shown in Fig. 4(b) so that the convergence can be seen more clearly. We compute the L^1 and L^∞ errors between the numerical solutions of the radiative transfer equation and the diffusion equation respectively in Fig. 5(a) and (b) , both of which display a good convergence as ϵ decreases.

Figs. 6 - 8 display the numerical results using interface condition II. There exists an interface layer with this interface condition, and the energy density $a(t,x,\mu)$ is no longer isotropic in the μ-direction, as can be seen from Fig. 6. Since the interface layer exists, we need more grid points (near the interface) to resolve ϵ such that $\Delta x \ll \epsilon$. This should be done locally near the interface, but we do not pursue this local adaptive mesh idea in this paper, instead we simply double the number of grid points by using $\Delta x = \Delta\mu = 1/400$. The time step is chosen as the same function of Δx as in interface condition I. Fig. 7 shows the result of the average density $\bar{a}(t,x)$ comparing with its diffusion limit with decreasing ϵ. Similarly to the case of interface condition I,

the good convergence can be observed here and more clearly in a zoomed-in image Fig. 7(b). An interface layer also can be seen in this figure, which does not exist with interface condition I (comparing with Fig. 4(b)). Finally, L^1 error between the numerical solutions of the radiative transfer and the diffusion equations is depicted in Fig. 8 for both meshes $\Delta x = 1/200$ and $\Delta x = 1/400$. One can see that the under-resolved errors do not become small when ϵ is reduced, however when we resolve ϵ, i.e. using a small enough Δx, the errors decrease as ϵ does. We can not have L^∞ convergence in this situation due to the existence of the interface layer.

Example 2 $\sigma_1(\mu, \mu') = \frac{1}{2}$, $\sigma_2(\mu, \mu') = 1$, $\Sigma_1 = 1$, $\Sigma_2 = 2$. *The initial condition of the radiative transfer equation (4.1) is given by*

$$a(0, x, \mu) = \begin{cases} 1, & x < 0, \mu > 0, \sqrt{4x^2 + 4\mu^2} < 1 \\ 1 & x > 0, \mu < 0, \sqrt{4x^2 + \mu^2} < 1, \\ 0 & \textit{otherwise}, \end{cases} \tag{5.3}$$

and the corresponding initial datum for the diffusion equation (4.9) is

$$\begin{aligned} a^{(0)}(0, x) &= \frac{1}{2} \int_{-1}^{1} a(0, x, \mu)\, d\mu \\ &= \begin{cases} \frac{1}{4}\sqrt{1 - 4x^2}, & -\frac{1}{2} < x < 0, \\ \frac{1}{2}\sqrt{1 - 4x^2}, & 0 < x < \frac{1}{2}, \\ 0, & \textit{otherwise}. \end{cases} \end{aligned} \tag{5.4}$$

Unlike the Gaussian initial data in Example 1, we use the discontinuous initial data (5.3) and (5.4) in this example. Two different constants are used for the scattering cross section σ_i in two domains. But it will not affect the value of α for both interface conditions. Hence α is the same as in the first example.

We use the same computational domain as the first example, namely $(x, \mu) \in [-3, 3] \times [-1, 1]$. Although the support set for x is $[-\frac{1}{2}, \frac{1}{2}]$ in the initial data here, we choose the domain of x to be $[-3, 3]$, which is big enough for the diffusion of $a(t, x, \mu)$ so the periodic boundary condition can be used in our computational time span.

The results show good performance of the scheme. Here we show the numerical convergence of the solutions from the radiative transfer equation to the diffusion equation in Fig. 9-11 for interface conditions I and II respectively. The interface layer can be seen more clearly in Fig. 10(b). In particular, the interface layer on the right of the interface is clearly visible in Fig.11(b) for the case of interface II, but it does not exist in Fig.11(a) in the case of interface I. both the L^1 and L^∞ convergences in ϵ still hold as before but will not be shown here since they are similar to Example 1.

In both examples we used piecewise constant coefficients ρ, v, σ and Σ to test the numerical performance of the new scheme. The scheme is valid for general variable coefficients for these quantities. Since the focus of the paper is to capture the correct behavior at the interface, we do not conduct numerical tests on more general variable coefficients, which do not introduce any new numerical challenge for a standard radiative transfer equation solver.

6 Conclusion

In this paper, we develop a numerical method to solve the plane symmetry, isotropic scattering radiative transfer equation with an interface that models the propagation of energy density of waves in heterogeneous media with weak random fluctuation. The numerical method follows the idea of [13, 15], namely, we build in the interface condition that characterizes the reflection and transmission into the numerical flux. The new contribution is to deal with the diffuse transmission that typically occurs in translucent media. Moreover, we compare its numerical solution with the numerical solution of the diffusion equation for both the regular and diffuse transmissions. The results show that, as the mean free path goes to zero, the numerical solutions of the radiative transfer equation with interface converges to those of the diffusion equation with the corresponding interface conditions under suitable numerical mesh sizes and time steps.

In the future we will attempt to develop numerical schemes for this problem that allows a coarse computation, in which the mesh size and time step are independent of the mean free path by combining the asymptotic-preserving scheme of [12] with the interface technique developed in this paper. We will also extend the method to higher dimensions, and with a curved interface [11].

References

[1] G.Bal, J.B.Keller, G.Papanicoalou and L. Ryzhik, Transport theory for acoustic waves with reflection and transmission at interfaces, *W*ave Motion, 30, 1999, 303-327.

[2] G. Bal and L. Ryzhik, Diffusion approximation of radiative transfer problems with interfaces, *Siam J. Appl. Math.*, Vol. 60, No. 6, pp. 1887-1912.

[3] G. Bal, G. Papanicolaou and L. Ryzhik, Diffusive energy scattering from weakly random surfaces, Journal of Mathematical Physics, 40, 1999, 4813-4827.

[4] Yu. Barabanenkov, Yu. Kravtsov, V. Ozrin and A. Saichev, Enhanced backscattering in optics, Progress in Optics 29, (1991), 67-190.

[5] C. Bardo, R. Santos and R. Sentis, Diffusion approximation and computation of the critical size, *Transactions of the American Mathematical Society*, Vol. 284, No.2(Aug.,1984), pp617-649.

[6] A. Bensoussan, J.L. Lions and G. Papanicolaou, Boundary layers and homogenization of transport processes, *J. Publ. of RIMS, Kyoto Univ.*, Kyoto, Japan, Vol. 15, 1 (1979) pp. 53-157.

[7] S. Chandrasekhar, **Radiative Transfer**, Dover publications,Inc. New York, 1960.

[8] R. Dautray and J. L. Lions, **Mathematical Analysis and Numerical Methods for Science and Technology**, Springer-Verlag, Berlin, 1993.

[9] F. Golse, S. Jin and C.D. Levermore, A domain decomposition analysis for a two-scale linear transport problem, *Math. Model Num. Anal.*, 37, 869-892, 2003.

[10] A. Ishimaru, **Wave propagation and scattering in random media**, Vol,1-2, Academic Press, New York, 1978.

[11] S. Jin and X. Liao, A Hamiltonian-preserving scheme for high frequency elastic waves in heterogeneous media, *J. Hyperbolic Diff Eqn.*, 3, No. 4, 741-777, 2006.

[12] S. Jin, L. Pareschi and G. Toscani, Uniformly Accurate Diffusive Relaxation Schemes for Multiscale Transport Equations , *SIAM J. Num. Anal.*, 38, 913-936, 2000 (electronic).

[13] S. Jin and X. Wen, Hamiltonian-preserving schemes for the Liouville equation with discontinuous potentials, *Comm. Math. Sci.*, 3, 285-315, 2005.

[14] S. Jin and X. Wen, Hamiltonian-preserving schemes for the Liouville equation of geometrical optics with discontinuous local wave speeds, *J. Comp. Phys.*, 214, 672-697, 2006.

[15] S. Jin and X. Wen, Hamiltonian-preserving schemes for the Liouville equation of geometrical optics with partial transmissions and reflections, *SIAM J. Num. Anal.*, 44, 1801-1828, 2006.

[16] S. Jin and X. Wen, Computation of Transmissions and Reflections in Geometrical Optics the Reduced Liouville Equation, *Wave Motion*, 43(8), 667-688, 2006.

[17] E. W. Larsen and J.B. Keller, Asymptotic solution of neutron transport problems for small mean free paths, *J. Math. Phys.*, 15(1974), pp.75-81.

[18] R.J. LeVeque, **Finite Volume Methods for Hyperbolic Problems**. Cambridge University Press, 2002.

[19] R.J. LeVeque and Z.L. Li, The immersed interface method for elliptic equations with discontinuous coefficients and singular sources, *SIAM J. Numer. Anal.*, 31, 1019–1044, 1994.

[20] R.J. LeVeque and C.M. Zhang, The immersed interface method for acoustic wave equations with discontinuous coefficients, *Wave Motion*, Vol.25, No.3, May 1997, 237-263(27).

[21] X.D. Liu, R. Fedkiw and M. Kang, A boundary condition capturing method for Poisson's equation on irregular domains, J. Comput. Phys. 160, 151-178, 2000.

[22] P.A. Markowich, C.A. Ringhofer, and C. Schmeiser, **Semiconductor Equations**, Springer-Verlag, Wien, 1990.

[23] A. Mayo, The fast solution of Poisson's and the biharmonic equations on irregular regions, SIAM J. Sci. Comput. 21, 285-299, 1984.

[24] A. Mayo, The rapid evaluation of volume integrals of potential theory on general regions, J. Comput. Phys. 100, 236-245, 1992.

[25] L. Ryzhik, G. Papanicolaou and J.B. Keller, Transport equations for elastic and other waves in random media. *Wave Motion*, 24(4):327-370, 1996.

[26] L. Ryzhik, G. Papanicolaou and J.B. Keller, Transport equations for waves in a half space. *C*omm. PDE's, 22, (1997), 1869-1910.

[27] X. Yang, F. Golse, Z.Y. Huang and S. Jin, Numerical study of a domain decomposition method for a two-scale linear transport equation, *Networks and Heterogeneous Media* 1(1), 143-166, 2006.

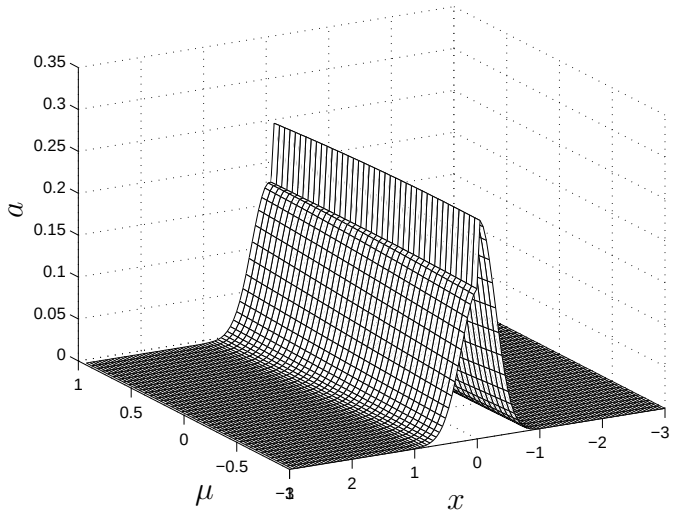

Figure 3: Example 1. The numerical solution of $a(t, x, \mu)$ for the radiative transfer equation (4.1) at $t = 0.1$, $\epsilon = 0.03$ using interface condition I. $\Delta x = \Delta\mu = 1/200$.

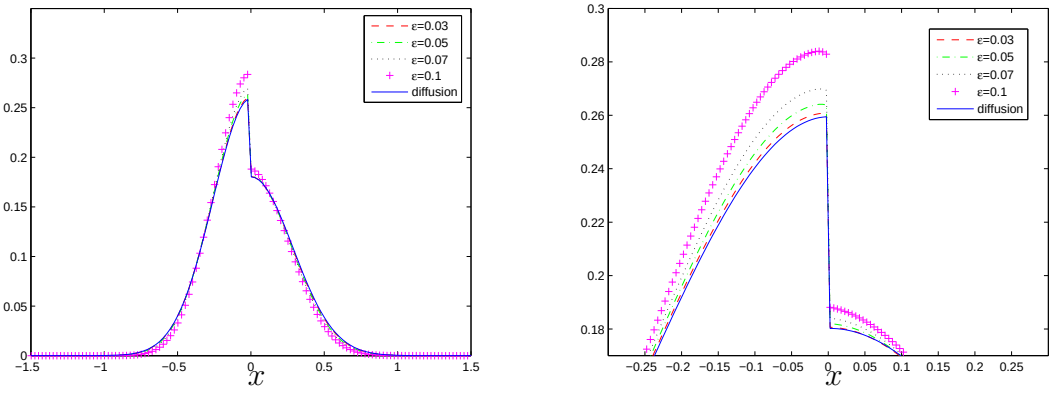

(a) Solution in domain $x \in [-1.5, 1.5]$

(b) Solution in domain $x \in [-0.3, 0.3]$

Figure 4: Example 1. The numerical solution of the average density $\bar{a}(t, x) = \frac{1}{2}\int_{-1}^{1} a(t, x, \mu)\, d\mu$ for the radiative transfer equation (4.1) converges to the numerical solution of $a^{(0)}$ for the diffusion equation (4.9) at $t = 0.1$ with ϵ decreasing from 0.1 to 0.03 using interface condition I. $\Delta x = \Delta\mu = 1/200$. A zoomed-in plot is shown in (b).

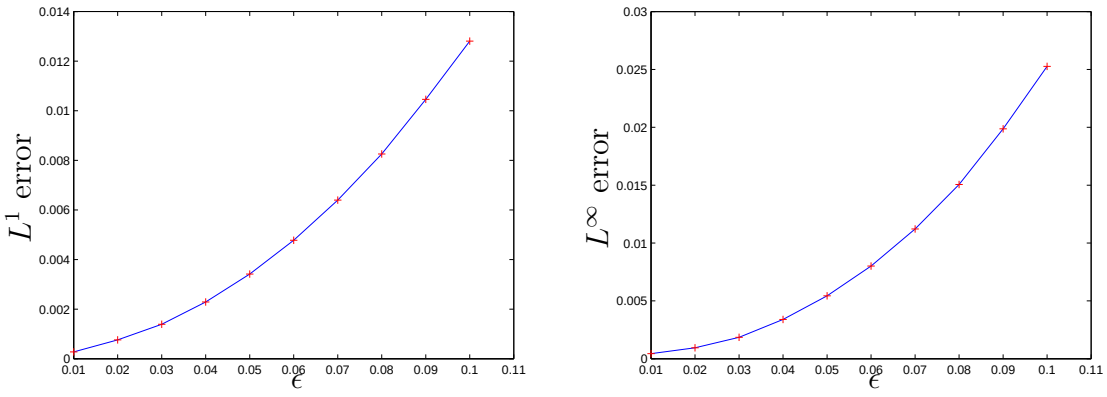

(a) L^1 convergence

(b) L^∞ convergence

Figure 5: Example 1. The L^1 error in (a) and L^∞ error in (b) between the numerical solutions of the radiative transfer equation and the diffusion equation when ϵ is decreasing from 0.1 to 0.01 using interface condition I.

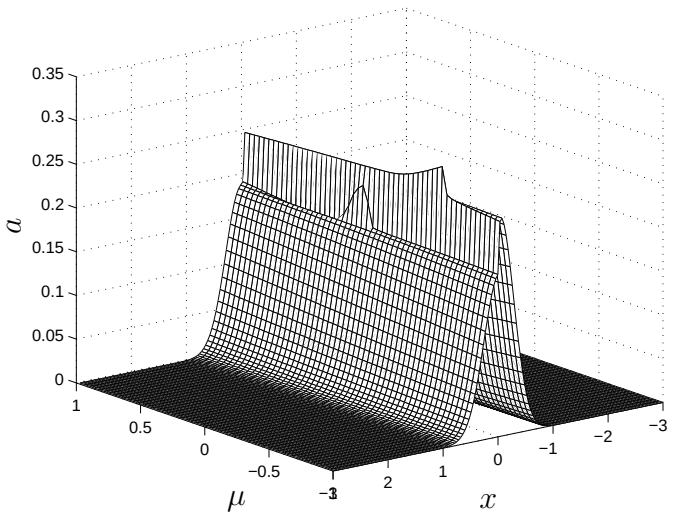

Figure 6: Example 1. The numerical solution of $a(t, x, \mu)$ for the radiative transfer equation (4.1) at $t = 0.1$, $\epsilon = 0.03$ using interface condition II. $\Delta x = \Delta\mu = 1/400$.

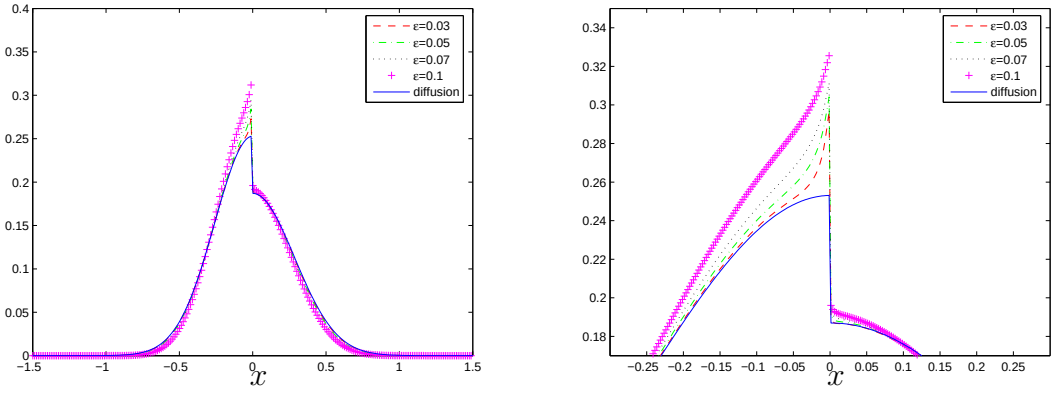

(a) Solution in domain $x \in [-1.5, 1.5]$ (b) Solution in domain $x \in [-0.3, 0.3]$

Figure 7: Example 1. The numerical solution of the average density $\bar{a}(t,x) = \frac{1}{2}\int_{-1}^{1} a(t,x,\mu)\,d\mu$ for the radiative transfer equation (4.1) converges to the numerical solution of $a^{(0)}$ of the diffusion equation (4.9) at $t = 0.1$ with ϵ decreasing from 0.1 to 0.03 using interface condition II. $\Delta x = \Delta\mu = 1/400$. A zoomed-in plot is shown in (b).

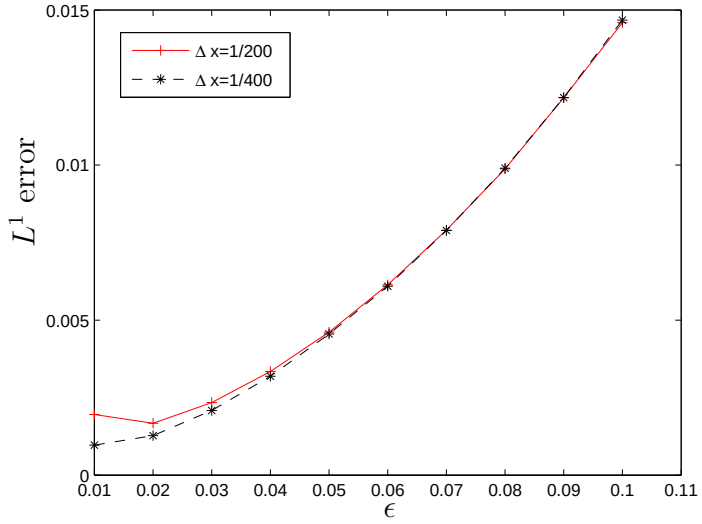

Figure 8: Example 1. The L^1 error between the numerical solutions of the radiative transfer equation and the diffusion equation when ϵ is decreasing from 0.1 to 0.01 using interface condition II.

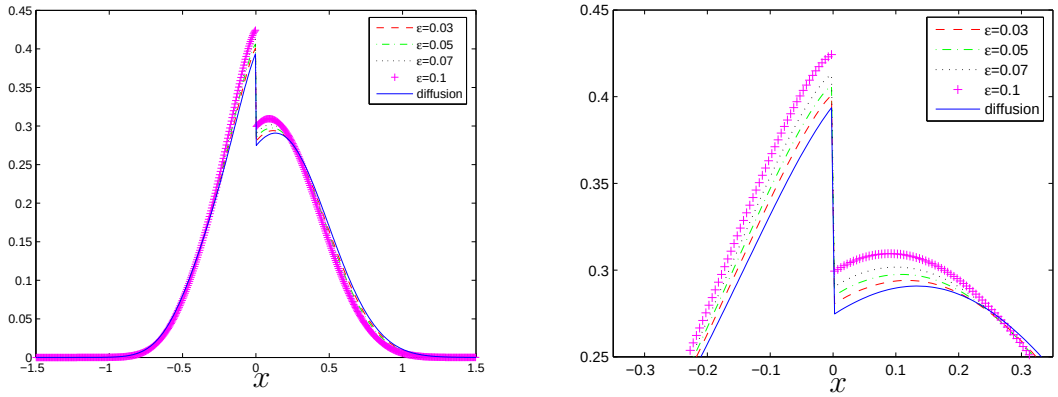

(a) Solution in domain $x \in [-1.5, 1.5]$ (b) Solution in domain $x \in [-0.35, 0.35]$

Figure 9: Example 2. The numerical solution of the average density $\bar{a}(t,x) = \frac{1}{2}\int_{-1}^{1} a(t,x,\mu)\,d\mu$ for the radiative transfer equation (4.1) converges to the numerical solution of $a^{(0)}$ for the diffusion equation (4.9) at $t = 0.1$ with ϵ decreasing from 0.1 to 0.03 using interface condition I. $\Delta x = \Delta\mu = 1/200$. A zoomed-in plot is shown in (b).

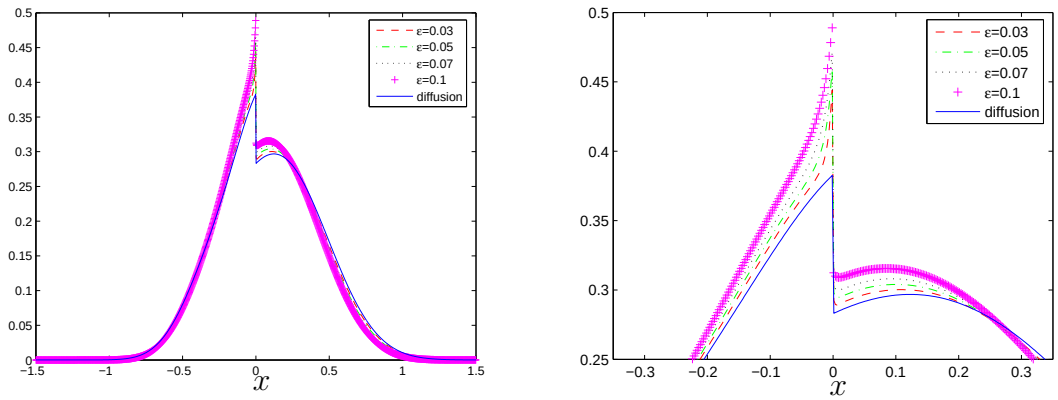

(a) Solution in domain $x \in [-1.5, 1.5]$ (b) Solution in domain $x \in [-0.35, 0.35]$

Figure 10: Example 2. The numerical solution of the average density $\bar{a}(t,x) = \frac{1}{2}\int_{-1}^{1} a(t,x,\mu)\,d\mu$ for the radiative transfer equation (4.1) converges to the numerical solution of $a^{(0)}$ for the diffusion equation (4.9) at $t = 0.1$ with ϵ decreasing from 0.1 to 0.03 using interface condition II. $\Delta x = \Delta\mu = 1/400$. A zoomed-in plot is shown in (b).

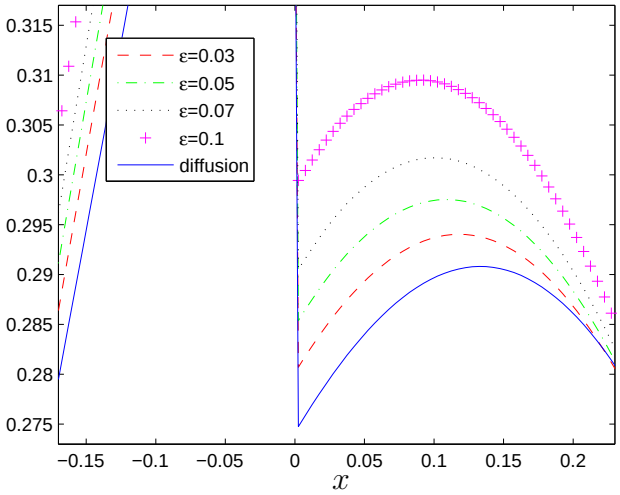

(a) Using interface condition I

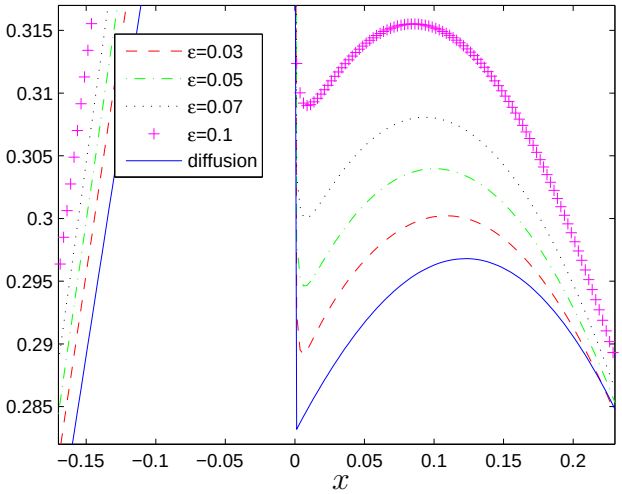

(b) Using interface condition II

Figure 11: Example 2. More zoomed-in plots: (a) is enlarged from Fig.9(a) and (b) is from Fig.10(a). This shows a comparison between the solution without the interface layer (a) for interface condition I and the solution with the interface layer(b) on the right of the interface with interface condition II.